

# Simulations of Matched-Field Processing in a Deep-Water Pacific Environment

MICHAEL B. PORTER, RONALD L. DICUS, AND RICHARD G. FIZELL

(Invited Paper)

**Abstract**—Conventional bearing estimation procedures employ plane-wave steering vectors as replicas of the true field and seek to resolve in angle by maximizing a power function representing the agreement between actual and replica fields. For vertical arrays in oceanic waveguides the received field depends on range and depth, and it is natural to replace the “look-direction” ( $\theta$ ) by a “look-position” ( $r, z$ ). Thus an environmental model is constructed by specifying ocean depth, sound speed profile, bottom properties, etc., and a propagation model is employed to construct a replica of the field that would be received on the array for a particular source position. The usual estimators (e.g., Bartlett or maximum likelihood) are then used to gauge the agreement between actual and replica fields and the true source position is identified as that position where the agreement is best. The performance of this kind of matched-field processing is strongly affected by the environment. In particular, we demonstrate through simulations that for a deep-water Pacific environment dominated by waterborne paths, ambiguities or sidelobes are associated with convergence zones. In the absence of mismatch between replica and actual fields we find that a 16-element array performs extremely well in low-frequency regimes. Mismatch caused by uncertainties in phone positions, bottom parameters, ocean sound speed, surface and bottom roughness, etc., causes degradation in localization performance. The impact of some of these effects on conventional and maximum likelihood estimators is examined through simulation.

## I. INTRODUCTION

**D**URING the last few years there has been an increasing interest in merging propagation models with signal processing algorithms to improve source detection and localization [1]–[9]. There are several approaches to this problem including back-propagation [3], [7], and mode separation procedures [8].

The approach employed in this paper is matched-field processing [1], [2], [5], [6], [9]. The matched-field processor takes the same form as traditional estimators such as the Bartlett (conventional) or maximum likelihood method (MLM) estimator except that the plane-wave replica vector is replaced by a replica vector derived from a propagation model for the oceanic waveguide which accounts for the refractive and multipath effects. Thus the “look-direction” ( $\theta$ ) is replaced by a “look-position” ( $r, z$ ) in range and depth. This procedure was introduced and demonstrated by Bucker [1] using simulated data in a shallow water environment. Heitmeyer *et al.* [2] subsequently performed more detailed

comparisons in a Pekeris waveguide. More recently, preliminary successes have been obtained with real data taken in the Arctic [6]. The success of this work has encouraged us to examine range-depth localization in another environment, specifically a deep-water Pacific environment.

The thrust of this paper is to demonstrate by simulations what factors are likely to affect the performance of such a procedure in an actual experiment. We suggest that an understanding of the physical aspects of the acoustic propagation is important in understanding the performance of the range-depth localization procedure. While the quantitative results are specific to our scenario it is hoped that the qualitative insights may be applied to more general cases.

The outline of this paper is as follows. In Section II we review the range-depth localization procedure. In Section III we illustrate the performance of the procedure in an idealized environment in which the propagation model is perfectly faithful to the actual environment. In Section IV we examine the degradation induced by mismatch caused by our inability to model the environment perfectly. Specifically, we look at degradation due to error in the ocean sound speed profile and subbottom properties. Finally, in Section V we end with a summary and conclusions.

## II. RANGE-DEPTH LOCALIZATION

Traditionally, source bearing is estimated by finding the maximum of a function given by (Bartlett or conventional estimator)

$$S(\theta) = e^*(\theta) \text{Re}(\theta)$$

where  $e(\theta)$  is a plane-wave replica field vector depending on the hypothetical bearing angle of the source and “\*” denotes the complex conjugate transpose. In addition,  $R$  is the cross-spectral matrix given by

$$R_{ij} = E[d_i d_j^*]$$

where  $d_i$  denotes the discrete Fourier transform of the received field on phone  $i$ . The discrete Fourier transform is performed at the CW frequency being used for localization and then  $E[\cdot]$  is calculated by averaging over a sequence of time frames. We also consider the Capon [10] estimator (MLM) given by

$$S(\theta) = 1/\{e^*(\theta)R^{-1}e(\theta)\}.$$

The natural generalization to range-depth ( $r, z$ ) localization

Manuscript received April 2, 1986; revised September 8, 1986.

The authors are with the Applied Ocean Research Branch, Naval Research Laboratory, Washington, DC 20375.

IEEE Log Number 8714260.

## ENVIRONMENT

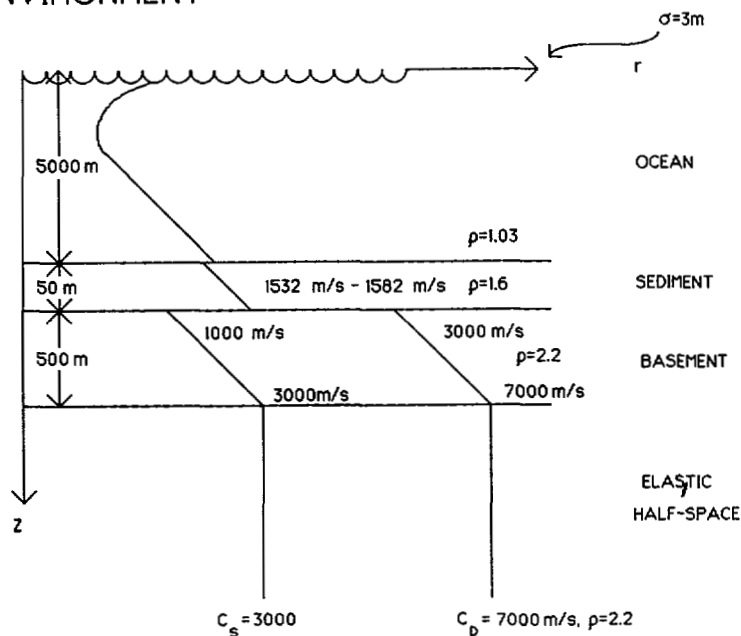


Fig. 1. Environmental model used for computing the field received on the array.

with a vertical array in a cylindrically symmetric oceanic waveguide simply requires that the plane-wave replica vector  $e(\theta)$  be replaced by  $e(r, z)$ , which must now be generated by a propagation model. There exist several procedures (fast field program, parabolic equation method, ray/beam tracing, normal modes,  $\dots$ ) which have different merits and have all been extensively described in the literature. The simulations described in this paper employ replica fields obtained by a normal mode program [11]. In addition, the  $d$  vector used to generate the cross-spectral matrix is also generated by the normal mode model, and a nonsingular cross-spectral matrix is obtained by adding a diagonal matrix representing white noise 10 dB below the signal.

The result of these computations is expressed by an ambiguity surface  $S(r, z)$  measuring the agreement between actual and replica fields  $e(r, z)$  over a domain of range and depth.

### III. IDEAL (NO MISMATCH) CASE

The environmental model used in these simulations is depicted schematically in Fig. 1. In these simulations with no mismatch, the actual and replica vectors are generated using the same environmental model. The sound speed profile in the ocean was obtained from archival data. The sediment has a sound speed profile (SSP) which increases linearly with depth with a gradient of 1.0/s and is 50 m thick. The subbottom (beneath the sediment) is modeled as an elastic medium with both  $P$ - and  $S$ -wave velocities increasing linearly with depth, to a depth of 5550 m beneath the ocean surface. Finally, the medium is terminated with a homogeneous half-space. The  $P$ - and  $S$ -wave speeds at the sediment/subbottom interface are 1000 and 3000 m/s, respectively, with corresponding gradients of 4 and 8 s. Attenuation of 0.05 dB/(km·Hz) has also

been included in  $S$ - and  $P$ -wave velocities. An RMS surface roughness of 3 m is incorporated using the Kuperman-Ingenito scatter model [12]. Thus the environmental model includes both bottom and surface-reflection loss. Finally, the source frequency in these simulations is 10 Hz.

Before examining the ambiguity surfaces, it is profitable to examine the synthetic field plots for this environment. In Fig. 2 we display the field power for a source depth of 250 m. In order to compensate for the limited number of gray scales, the field has been scaled in range by a factor of  $r$  to remove the cylindrical spreading loss. Fig. 2(a) includes only the waterborne modes, which we define as modes with phase velocity less than the ocean sound speed velocity at the ocean/sediment interface. The familiar convergence zone (CZ) pattern with energy cycling up and down the channel is manifest. In Fig. 2(b) we have included the bottom-interacting modes, the effect of which is the filling in of some of the shadow zones. Bottom-interacting modes with the real part of their phase velocity less than 15 000 m/s have been included. These include a number of leaky modes, and based on comparisons with the exact spectral integral representation (i.e., the FFP or reflectivity method), should be adequate to describe the field beyond a few kilometers in range. Collectively, the two plots are a reminder of which ray take-off angles are important at which ranges.

We next consider the source localization problem in this environment. A vertical array of 16 phones was placed in the shadow zone (SZ) at a range of 25 km. The individual phones were spaced every 62.5 m so that the deepest phone was located at a depth of 1000 m. Fig. 3 shows a sequence of range-depth ambiguity surfaces for this scenario. Note that the gray scale employs a nonconstant spacing between levels and the ambiguity surface has been normalized so that its maximum is unity. Fig. 3(a) and (b) was obtained using a

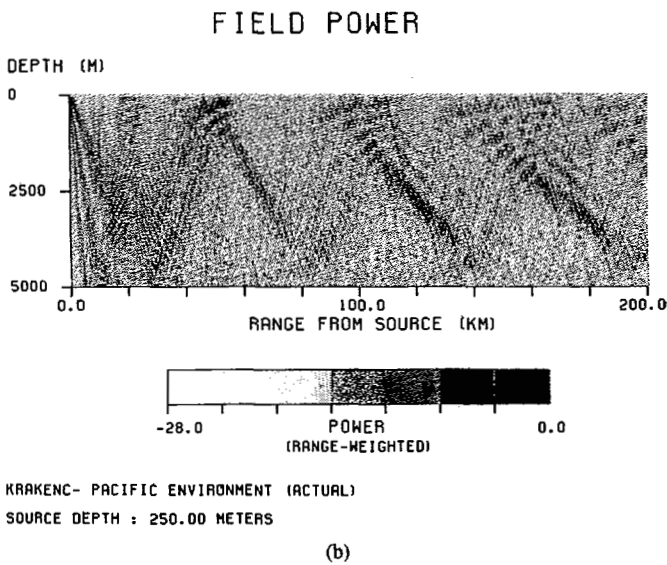
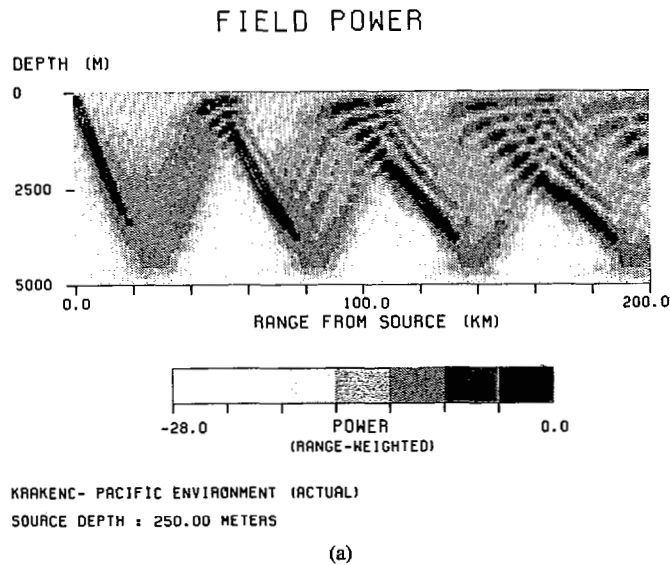


Fig. 2. Field power for a source at a depth of 250 m (a) including only waterborne modes, and (b) including bottom-interacting modes with a phase speed of less than 15 000 m/s.

conventional and MLM estimator, respectively, using only the waterborne energy for constructing both the actual and replica fields. The conventional estimator has sufficiently high side-lobes so as to obscure the true source position. In contrast, the MLM estimator clearly distinguishes the source. While these results cast the MLM estimator in a good light, it should be borne in mind that the maximum of the conventional estimator still occurs at the correct position.

The next scenario was designed to examine whether there are significant differences when the array is in the shadow zone and when the array is in the convergence zone. The array was moved out to the second convergence zone at 100-km range, and the same two ambiguity surfaces (conventional and MLM estimators) are shown in Fig. 3(c) and (d). Note that the range is four times larger in these surfaces, which sometimes gives a false impression of higher range resolution. We observe that the ambiguity surface in Fig. 3(c) reflects the periodicity of the waterborne field. This is expected since if we examine the field plot in Fig. 2(a) we see that the field that

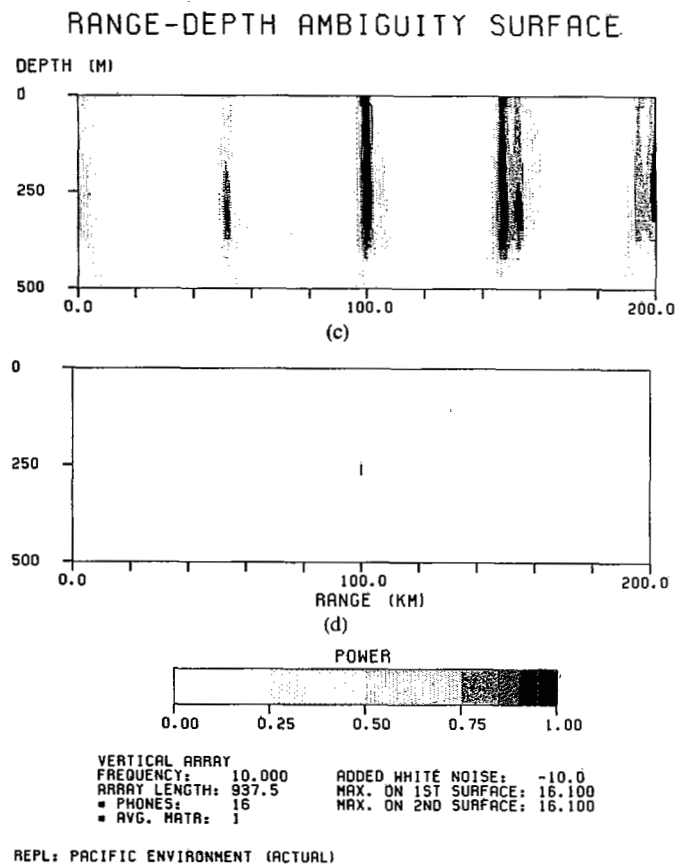
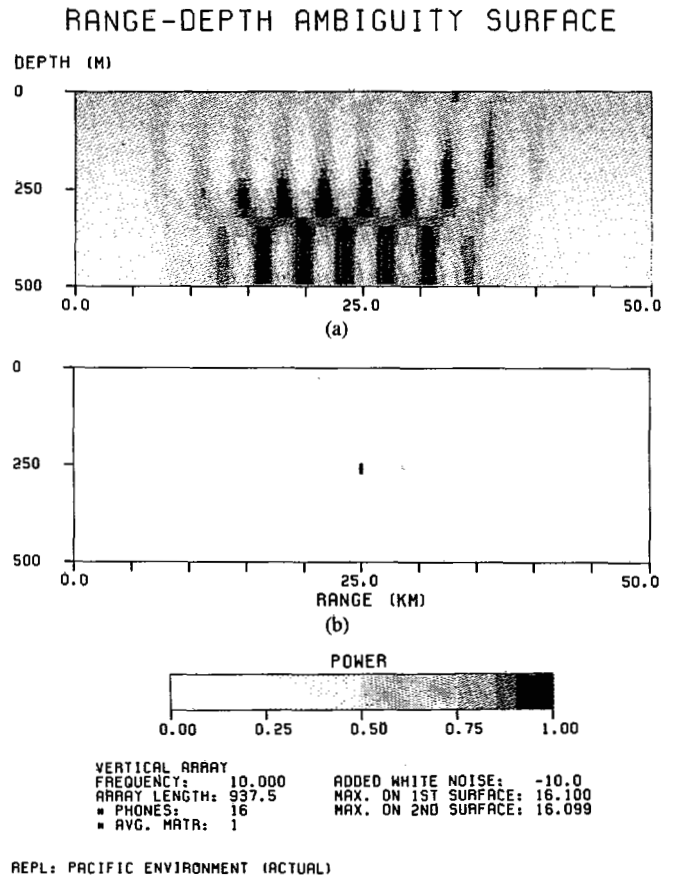


Fig. 3. (a) Conventional and (b) MLM ambiguity surfaces for a source at 250-m depth and 25-km range using only the waterborne modes. (c) and (d) Corresponding surfaces for a source at 100-km range.

would be received on such a vertical array at 100 km is "similar" to that which would be received at the next cycling at around 150 km, and so on. It is also clear that adjacent cycles are more similar than well-separated cycles. Of course, similarity to the eye does not guarantee similarity in the estimator, especially since phase information is available to the estimator which is not shown in the field amplitude plots.

When bottom-interacting modes are included in both actual and replica we obtain the sequence in Fig. 4. (The sequence of conventional and MLM for the shadow zone source and convergence zone source is repeated throughout the remainder of this paper.) The ambiguity surfaces for both the shadow zone source and the convergence zone source are significantly improved by the inclusion of these steeper ray paths. The bottom-interacting energy evidently eliminates the simple repetition in Fig. 4(c) and (d) by introducing detail in the pressure surface which helps distinguish one ray cycle from the next. In general, the field plot is much less structured, and it is more difficult to inspect the field plot and infer where high sidelobes will show up. The conventional estimator does, however, retain a hint of the CZ repetitions but, in general, is much sharper than before. The MLM surface again provides a much clearer picture of the true source location. In comparison to the nearer source it may be seen that the bottom-interacting energy makes a greater difference to the array in the shadow zone than to the array in the convergence zone.

The case where there is no mismatch is artificial; however, it provides an upper bound on performance as well as yielding some qualitative information. At higher frequencies or greater ranges the bottom-interacting energy is diminished, and we may expect to have difficulty resolving the successive cycles of the waterborne energy.

IV. EFFECTS OF MISMATCH

We first consider the problem of mismatch in subbottom properties. We presume that the environment described above is the actual environment and that bottom properties used for generating the replica vectors are in error. Specifically, the environment used for the replica vectors employs *P*- and *S*-wave speeds increased to 1200 and 3200 m/s at the sediment/subbottom interface and gradients increased to 5 and 9 s, respectively.

The usual sequence of ambiguity surfaces obtained using a conventional and MLM estimator is shown for a source at a range of 25 km and 100 km in Fig. 5. These are the same cases considered above, with the array in a deep shadow at 25 km and in the convergence zone at 100 km. In the shadow region, there are no "reliable acoustic paths" (refracted-refracted paths) connecting the source and receiver. Energy is partitioned between surface-reflected and bottom-reflected energy (of various orders), and the bottom mismatch has caused sufficient error in the replica vectors that the ambiguity surface possesses false peaks. In contrast, when the array is in the convergence zone at 100 km, the replica field for the true source position is less affected (since waterborne paths are proportionally more important), and the ambiguity surface is less degraded by the mismatch. In practice one might expect a decreased signal-to-noise ratio in the shadow zone, which

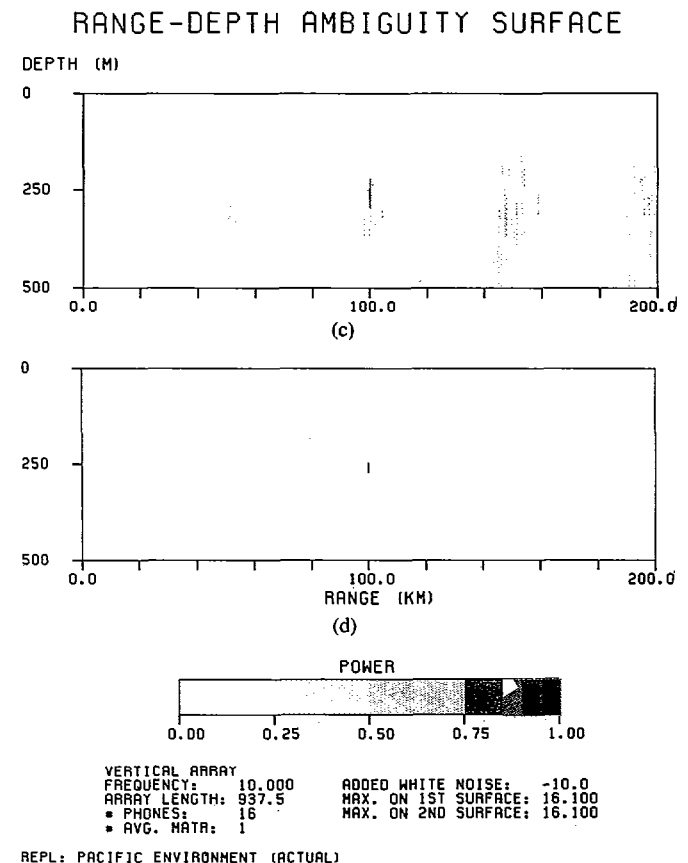
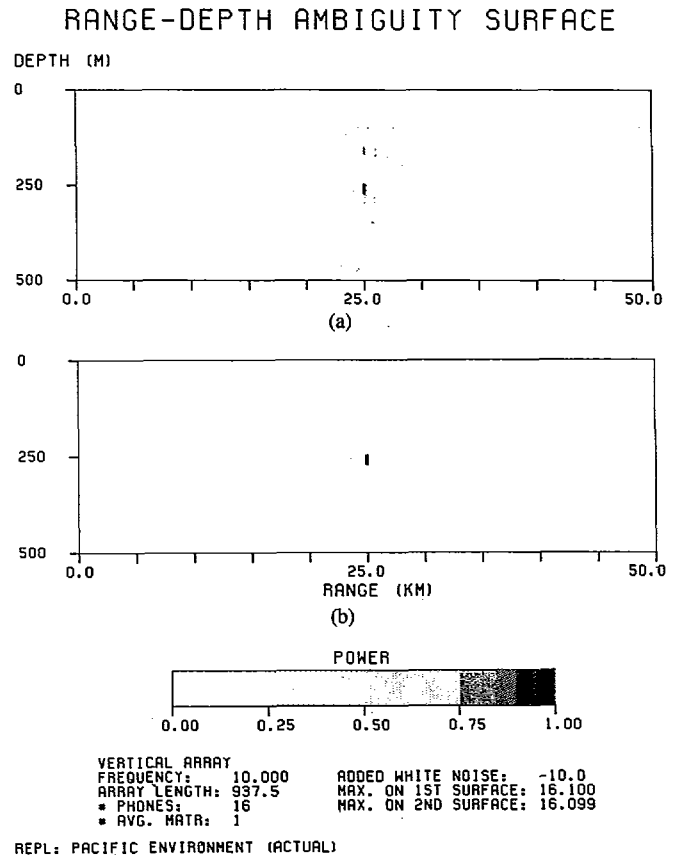


Fig. 4. Effect of including wide-angle ray paths for source at depth 250 m and range 25 km. (a) Conventional. (b) MLM and 100-km source range. (c) Conventional. (d) MLM.

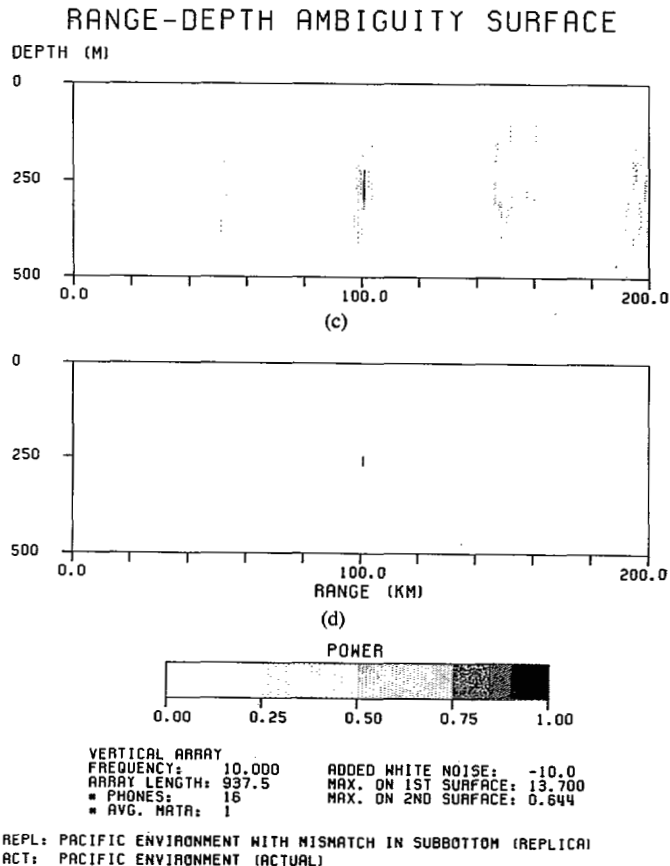
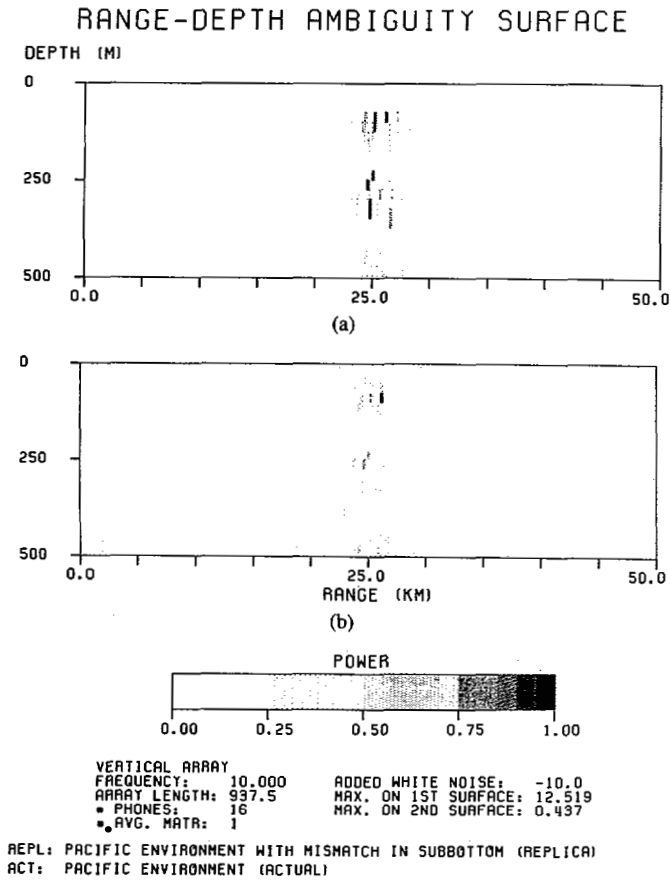


Fig. 5. Effect of mismatch in bottom properties for source at depth 250 m and range 25 km. (a) Conventional. (b) MLM and 100-km source range. (c) Conventional. (d) MLM.

would further favor localization performance in the CZ or direct path regimes.

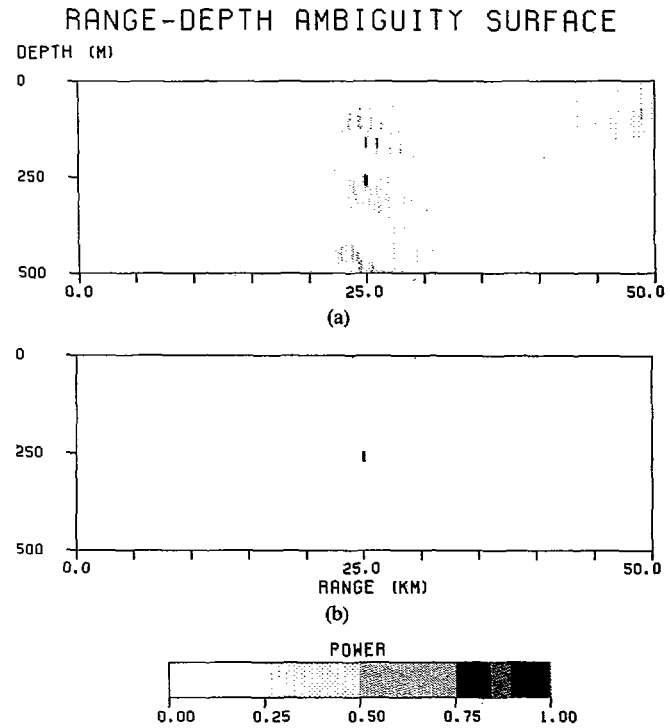
The role of ocean sound-speed errors is demonstrated in Fig. 6. In order to separate the effects of bottom-model and ocean-model errors we have removed the bottom mismatch. The sound speed profile has been increased by adding a linear function of the form  $\Delta c(z) = \delta(D - z)/D$  m/s within the water column. In Fig. 6 we have employed  $\delta = 2$  so that at the surface the sound speed is increased by 2 m/s, while at the ocean/sediment interface (and below) there is no change. The actual and replica fields include the bottom-interacting modes. The conventional (Fig. 6(a)) and MLM (Fig. 6(b)) ambiguity surfaces corresponding to the nearer source at 25 km show very little degradation caused by this mismatch. Both the conventional and MLM estimators obtain the correct cell for the source range and depth. In contrast, when the source range is moved out to 100 km, both estimators obtain their maximum at the next order CZ beyond the true source position as seen in Fig. 6(c) and (d).

At a particular range, this kind of error in SSP measurement is unlikely. On the other hand, even greater mismatch might occur if there is significant range variation in the SSP caused by, perhaps, eddies or up/downwelling. If the range dependence of the environment is sufficiently well known, then in these circumstances there may well be an advantage to employing a range-dependent model such as the parabolic equation method or ray/beam tracing. Unfortunately, these range-dependent models generally have other shortcomings, such as being restricted to acoustic (nonelastic) subbottoms or being inaccurate at low frequencies.

We next consider the role of uncertainty in sediment thickness. Sediment thickness is typically measured with an accuracy in these areas of no better than 50 m. A second cause of mismatch in sediment thickness is due to the variation in sediment thickness with range. In an abyssal hills environment, typical of vast regions of the Pacific, the sediment is roughly conformal with the underlying basement rocks, but tends to be thicker in troughs than on caps. The underlying basement is undulating with a wavelength of about 10 km and a waveheight of about 200 m. Thus a range-independent model has an intrinsic source of mismatch. The replica scenario employed to assess this effect is identical to the "actual" environment except that the sediment thickness has been increased to 100 m using the same sediment gradient and preserving the thickness of the other layers.

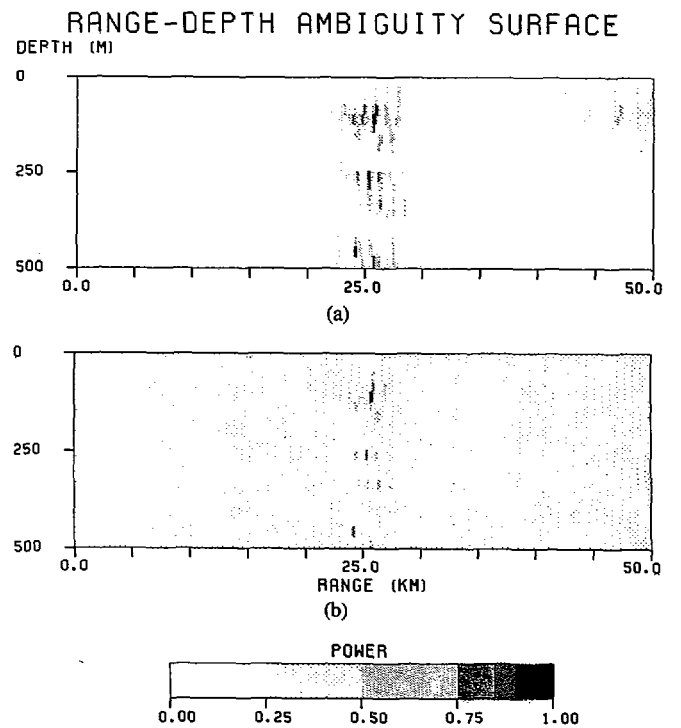
Fig. 7(a) and (b) shows the conventional and MLM surfaces for the nearer source at 25-km range and 250-m depth. We see that both surfaces have experienced some degradation generally comparable to that induced by the mismatch in subbottom wavespeeds previously considered. Based on the previous simulations we expect that the CZ source will be better localized, and this is verified in Fig. 7(c) and (d). The source is at 100 km and as usual, Fig. 7(c) is the conventional and 7(d) the MLM estimator.

Finally, we consider the role of source depth in matched-field processing. An omnidirectional source partitions its energy into waterborne and bottom-interacting energy (shallow- and wide-angle ray paths). In a range-independent



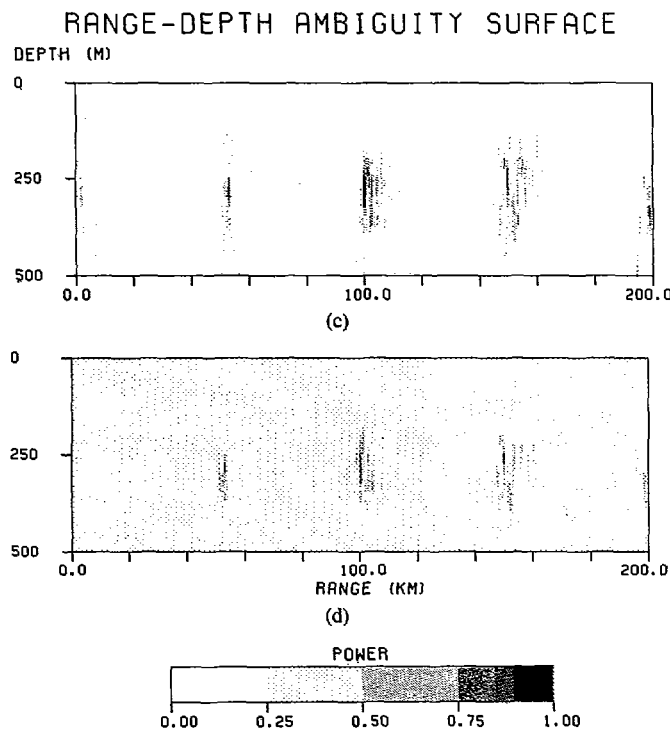
VERTICAL ARRAY  
 FREQUENCY: 10.000      ADDED WHITE NOISE: -10.0  
 ARRAY LENGTH: 937.5      MAX. ON 1ST SURFACE: 15.335  
 \* PHONES: 16              MAX. ON 2ND SURFACE: 1.862  
 \* AVG. MATR: 1

REPL: PACIFIC ENVIRONMENT WITH MISMATCH IN OCEAN SSP (REPLICA)  
 ACT: PACIFIC ENVIRONMENT (ACTUAL)



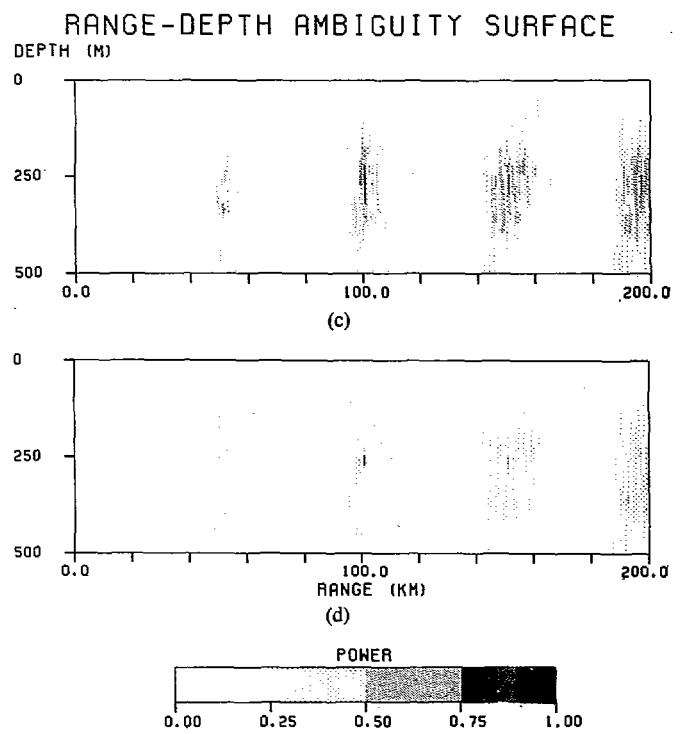
VERTICAL ARRAY  
 FREQUENCY: 10.000      ADDED WHITE NOISE: -10.0  
 ARRAY LENGTH: 937.5      MAX. ON 1ST SURFACE: 12.231  
 \* PHONES: 16              MAX. ON 2ND SURFACE: 0.406  
 \* AVG. MATR: 1

REPL: PACIFIC ENVIRONMENT WITH MISMATCH IN SEDIMENT (REPLICA)  
 ACT: PACIFIC ENVIRONMENT (ACTUAL)



VERTICAL ARRAY  
 FREQUENCY: 10.000      ADDED WHITE NOISE: -10.0  
 ARRAY LENGTH: 937.5      MAX. ON 1ST SURFACE: 11.703  
 \* PHONES: 16              MAX. ON 2ND SURFACE: 0.358  
 \* AVG. MATR: 1

REPL: PACIFIC ENVIRONMENT WITH MISMATCH IN OCEAN SSP (REPLICA)  
 ACT: PACIFIC ENVIRONMENT (ACTUAL)



VERTICAL ARRAY  
 FREQUENCY: 10.000      ADDED WHITE NOISE: -10.0  
 ARRAY LENGTH: 937.5      MAX. ON 1ST SURFACE: 13.175  
 \* PHONES: 16              MAX. ON 2ND SURFACE: 0.532  
 \* AVG. MATR: 1

REPL: PACIFIC ENVIRONMENT WITH MISMATCH IN SEDIMENT (REPLICA)  
 ACT: PACIFIC ENVIRONMENT (ACTUAL)

Fig. 6. Effect of mismatch in ocean sound speed profile for source at depth 250 m and range 25 km. (a) Conventional. (b) MLM and 100-km source range. (c) Conventional. (d) MLM.

Fig. 7. Effect of mismatch in sediment thickness for source at depth 250 m and range 25 km. (a) Conventional. (b) MLM and 100-km source range. (c) Conventional. (d) MLM.

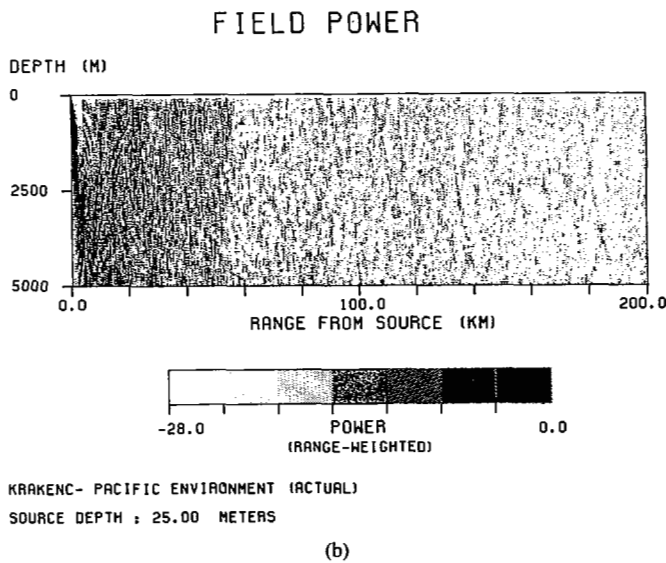
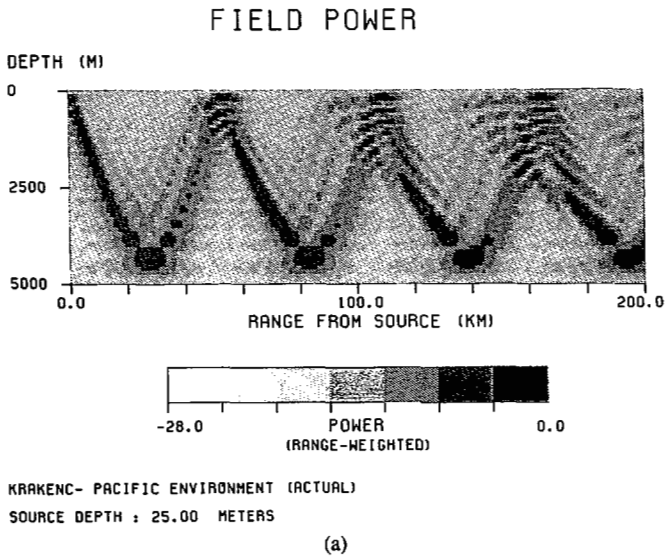


Fig. 8. Field power for a source at a depth of 25 m (a) including only waterborne modes and (b) including bottom-interacting modes with a phase speed of less than 15 000 m/s.

environment the limiting ray angle is determined by Snell's law and increases as the source depth moves toward the sound speed minimum. Thus a source at this minimum is imparting proportionally more energy into waterborne rays, and in an average (over space) sense one would expect better performance. We consider an extreme case where the source has been moved very close to the surface (source depth of 25 m). The field obtained by including only waterborne paths (Fig. 8(a)) retains the usual cyclic pattern; however, when bottom-interacting modes are included, the acoustic field is completely dominated by the bottom-interacting modes, and the CZ pattern is no longer visible (Fig. 8(b)). (In regions with greater bottom loss, the CZ pattern would be expected to persist better.) The ambiguity surfaces in Fig. 9 employ a replica field with the previously described mismatch in elastic wave speeds, and both waterborne and bottom-interacting modes are included. Not surprisingly, the localization performance is poor at both 25 and 100 km since the poorly matched bottom-interacting paths dominate the field.

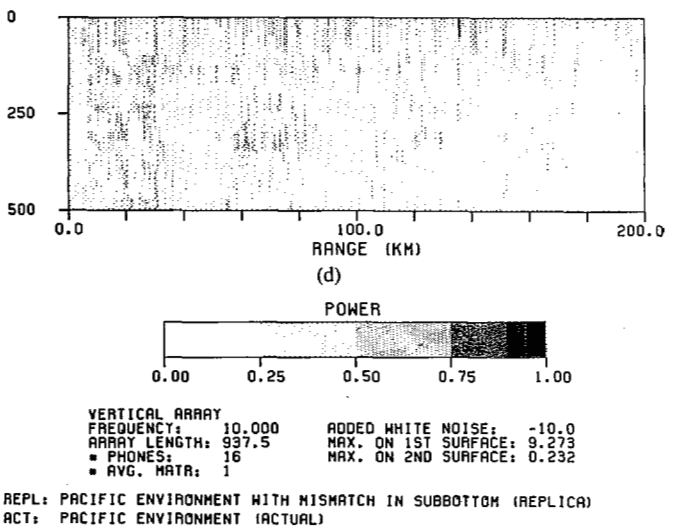
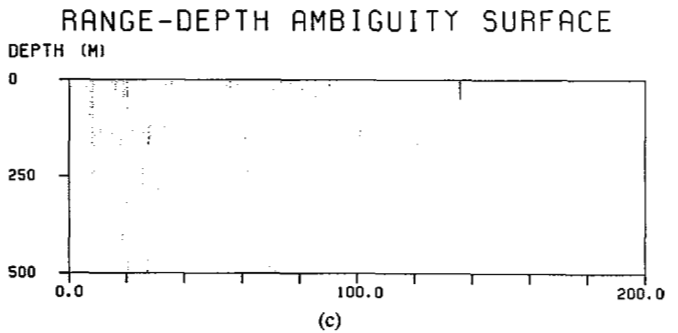
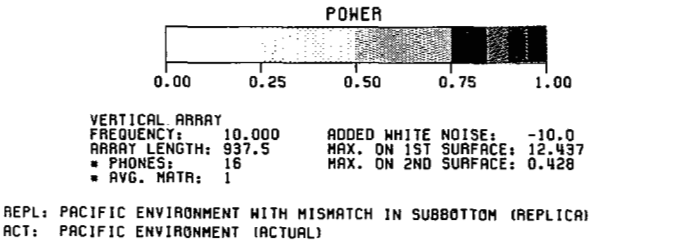
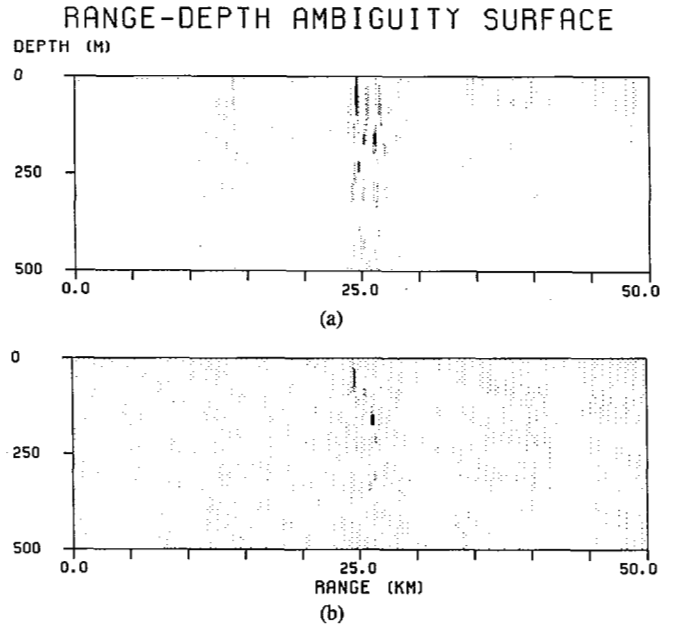


Fig. 9. Effect of mismatch in bottom properties for source at depth 25 m and range 25 km. (a) Conventional. (b) MLM and 100-km source range. (c) Conventional. (d) MLM.

For a specific source/receiver separation, a correlation between proximity to the SSP minimum and localization performance need not hold since changing the source depth changes both the strength and the positions of caustics or focusing regions. One can imagine a scenario where a particular array is in a CZ for a shallow source and not in the CZ for a deeper source located in the sound speed minimum.

## V. SUMMARY AND CONCLUSIONS

Localization performance of a matched field processor depends on the environment in which it is to be applied. This environment includes the water column sound velocity and properties of the boundaries. Although sound velocity in the water column can be accurately measured, bottom properties are less well known and predictions of performance are subject to this uncertainty. Bottom properties that must be specified include compressional and shear wave speeds, densities, and attenuations as a function of depth. Even this stratified model of the bottom departs significantly from what is known about abyssal hills provinces of the Pacific. In reality, roughness and three-dimensional spatial variations accompany the sedimentary and lithologic processes of oceanic crust building.

With this caveat in mind we have simulated matched field processing in a stratified environment that represents, to the best of our knowledge, average properties to be expected. The model environment included a typical Pacific sound speed profile, and a thin (50 m) sediment layer overlying an elastic layer (500 m thick) with linearly increasing wave speeds. Simulations were shown for ranges of 25 and 100 km and source depths of 25 and 250 m.

The first result is that the ambiguity surface shows excellent localization properties when the data and replica fields are identical. When the model fields were truncated to eliminate bottom-interacting modes, the peak of the conventional estimator spread out into a large range-depth cell when the receiver was in the shadow zone (SZ). In the convergence zone (CZ) localization was much less sensitive to the removal of bottom-interacting modes. This is to be expected since the CZ is dominated by waterborne energy, whereas the SZ is filled in with bottom-interacting energy. In the CZ, ambiguities occur at the ranges of other CZ orders although the maximum peak occurs at the correct range.

Matched field ambiguity surfaces are sensitive to mismatch between the true environment and the model environment. Since bottom properties cannot be routinely measured *in situ* as sound velocity profiles can, no prediction of performance can be made without consideration of environmental uncertainties. It was found that uncertainty in sound speed profile as simulated with a mismatch linearly increasing to 2 m/s at the surface caused very little degradation for the nearer source. Localization performance of the more distant source was, however, significantly degraded, presumably reflecting the cumulative effects of the SSP mismatch.

Uncertainty in bottom properties is itself a subject for discussion. Studies [13] of the upper crust suggest departures from more traditional geophysical measurements of deep oceanic basalt, and estimates of uncertainty are based on that work. Simulations with the mismatch in bottom properties

exhibited much greater performance degradation in the SZ than in the CZ. An examination of the field plots led us to an interpretation of which source/receiver positions gave the best ambiguity surfaces based on which ray paths would be expected to be most reliable. In a CZ-dominated scenario, performance was seen to be best where the more reliable waterborne ray paths dominated (in the CZ) and ambiguities or sidelobes were seen at successive cycles of the waterborne rays. Changes in sediment thickness had a similar effect.

Simulations with a near-surface source at 25-m depth showed poor localization performance in both the SZ and CZ when mismatch in the subbottom was included. An examination of the field plot revealed that the unreliable bottom-interacting energy dominated the field so that CZ cycling was difficult to detect.

In comparing the different estimators, we saw that the MLM estimator generally provided much reduced sidelobe levels when the same vertical scale was employed. Both estimators tended to give the same maximum location; however, when a false peak was identified, the MLM estimator would often still give a very sharp single peak.

In summary, matched field processing is a promising procedure for range-depth localization; however, it appears that improved measurement accuracy of ocean bottom properties or better signal processing schemes are needed for robust performance. This might include array presteering and broadband processors. The various kinds of mismatch considered in these simulations were shown to be of varying importance depending on the specific source/receiver geometry. Other causes of mismatch should be investigated, such as Doppler and scattering.

## ACKNOWLEDGMENT

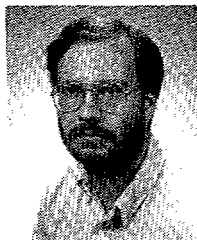
The authors wish to thank D. Cole for his assistance in performing the simulations.

## REFERENCES

- [1] H. P. Bucker, "Use of calculated sound fields and matched-field detection to locate sound sources in shallow water," *J. Acoust. Soc. Amer.*, vol. 59, p. 368, 1976.
- [2] R. M. Heitmeyer, W. B. Moseley, and R. G. Fizell, "Full field ambiguity function processing in a complex shallow-water environment," in *High Resolution Spatial Processing in Underwater Acoustics*, R. A. Wagstaff and A. B. Baggeroer, Eds. Washington, DC: GPO, 1985-570-276, pp. 171-191.
- [3] L. Nghiem-Phu, F. D. Tappert, and S. C. Daubin, "Source localization by CW acoustic retrogradation," unpublished, 1986.
- [4] R. Klemm, "Range and depth estimation by line arrays in shallow water," *Signal Process.*, vol. 3, pp. 333-344, 1981.
- [5] C. Zala, I. Barrodale, and M. Greening, "Investigation of algorithms for locating an acoustic source in shallow water," Victoria, B.C., Canada, Defence Research Establishment Pacific, Rep. 85-11, 1986.
- [6] R. G. Fizell and S. Wales, "Source localization in range and depth in an Arctic environment," in *Proc. 110th Meeting Acoustical Society America*, Suppl. 1 (Nashville, TN), vol. 78, 1985.
- [7] J. Perkins, private communication, 1985.
- [8] E. C. Shang, C. S. Clay, and Y. Y. Wang, "Passive source ranging by using mode filtering and mode phase comparing in waveguides," *J. Acoust. Soc. Amer.*, vol. 64, p. S118, 1983.
- [9] R. G. Fizell, "Application of high-resolution processing to range and depth estimation using ambiguity function methods," submitted to *J. Acoust. Soc. Amer.*
- [10] J. Capon, "High-resolution frequency-wavenumber spectrum analysis," *Proc. IEEE*, vol. 57, pp. 1408-1418, 1969.
- [11] M. B. Porter and E. L. Reiss, "A numerical method for bottom

interacting ocean acoustic normal modes," *J. Acoust. Soc. Amer.*, vol. 77, no. 5, pp. 1760-1767, 1985.

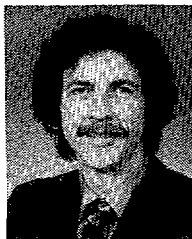
- [12] W. A. Kuperman and F. Ingenito, "Attenuation of the coherent component of sound propagating in shallow water with rough boundaries," *J. Acoust. Soc. Amer.*, vol. 61, no. 5, pp. 1178-1187, 1977.
- [13] O. I. Diachok, R. L. Dicus, and S. C. Wales, "Elements of a geoacoustic model of the upper crust," *J. Acoust. Soc. Amer.*, vol. 75, no. 2, p. 324, 1984.



**Michael B. Porter** was born in Quebec, Canada, on September 19, 1958. He received the B.S. degree in applied mathematics from the California Institute of Technology, Pasadena, in 1979. In 1984 he received the Ph.D. degree in engineering science and applied mathematics from Northwestern University, Evanston, IL.

From December 1983 to April 1985 he was a Scientist at the Naval Ocean Systems Center, San Diego, CA, where he performed research in numerical modeling of antennas, optical fibers, sonar transducers, and ocean acoustics problems. Since April 1985 he has been employed as a Research Physicist at the Naval Research Laboratory, Washington, DC. At NRL his interests have included matched-field processing and numerical modeling of wave propagation problems.

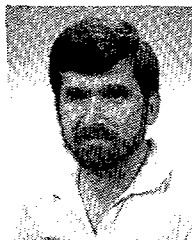
Dr. Porter is a member of the Acoustical Society of America.



**Ronald L. Dicus** was born in Baltimore, MD, on September 3, 1942. He received the B.S. degree in electrical engineering in 1965 from Drexel University, Philadelphia, PA. In 1972 he received the M.S. and Ph.D. degrees in physics from Rensselaer Polytechnic Institute, Troy, NY.

In 1972 he was employed as a Physicist in the Acoustical Oceanography Division of the Naval Oceanographic Office. His research was concerned with underwater acoustic propagation and acoustic interaction with the ocean bottom. In 1977 he took a Research Physicist position with the Naval Research Laboratory (NRL). In 1983 he became Supervisory Research Physicist and Head of the Boundary Effects and Ambient Noise Section within the Acoustics Division. Since joining NRL his interests have continued in acoustic bottom interaction as well as ambient noise, array performance modeling, Arctic acoustics, signal processing, and, more recently, the development of matched field processing techniques for real ocean environments.

Dr. Dicus is a member of the Acoustical Society of America.



**Richard G. Fizell** was born in Philadelphia, PA, on February 21, 1947. He received the B.S. degree from Drexel University, Philadelphia, PA, in 1969, the M.A. degree from the State University of New York, Stony Brook, in 1970, and the Ph.D. degree from Drexel in 1976, all in physics.

From 1969 until 1978, he worked for the U.S. Naval Air Development Center, Warminster, PA, planning and designing electronics systems for anti-submarine-warfare aircraft. He was on the faculty of Baptist College, Charleston, SC, in 1978-1979, and was at Ottawa University, Ottawa, KS from 1979 to 1982. In 1982 he joined the Applied Ocean Acoustics Branch at the Naval Research Laboratory, Washington, DC, where his interests include high-resolution signal processing and matched-field processing.

Dr. Fizell is a member of the Acoustical Society of America.